Chemical Engineering Journal 485 (2024) 149836

Contents lists available at ScienceDirect

Chemical Engineering Journal

journal homepage: www.elsevier.com/locate/cej

Pseudo-photoelectric cascade conversion endowing photosensitive Janus ionogel for solar energy harvesting and sensing

Jiale Sun [a,b], Yanan Liu [a,b], Junjie Wei [a,b,*], Peng Wei [d], Tao Chen [a,b,c,*]

[a] Key Laboratory of Marine Materials and Related Technologies, Zhejiang Key Laboratory of Marine Materials and Protective Technologies, Ningbo Institute of Material Technology and Engineering, Chinese Academy of Sciences, Ningbo 315201, China
[b] School of Chemical Sciences, University of Chinese Academy of Sciences, 19A Yuquan Road, Beijing 100049, China
[c] College of Material Chemistry and Chemical Engineering, Key Laboratory of Organosilicon Chemistry and Material Technology, Ministry of Education, Hangzhou Normal University, Hangzhou 311121, Zhejiang, China
[d] Department of Plastic and Reconstructive Surgery, Ningbo First Hospital, Ningbo 315010, China

ARTICLE INFO

Keywords:
Ionogel
Solar energy
Self-powered sensing
Cascade conversion
Pseudo-photoelectric effect

ABSTRACT

Ionic conductive gel based self-powered sensor has attracted much attention in Internet of Things era, due to its softness, versatility, electrical conductivity, iontronics and responsiveness. However, its multi-scene application is limited by few types of these perceptible signals. Herein, a photosensitive Janus ionogel with pseudo-photoelectric effect based on cascade conversion is reported, with seebeck coeffect of 19.5 mV K^{-1} and ZT value of 0.63. Significantly, the photosensitive Janus ionogel can generate different temperature gradients on the different intensity of sunlight, and convert solar energy into electric energy by the "light-thermal-electric" cascade conversion, demonstrating its great potential in solar energy utilization and light sensing. This investigation paves a promising and versatile way to construct photosensitive conductive materials for next-generation solar self-powered devices.

1. Introduction

To usher in the Internet of Things era, sensing materials and technologies, which are the foundation of the Internet of everything, have received continuous attention and vigorous development [1–4]. Taking into account the dependence of traditional sensors on external power sources during daily operation, self-powered characteristics are expected to be introduced into the sensor by integrating or coupling energy generating or harvesting function with the sensing function [5–8]. Benefitting from the advantages in terms of miniaturization, flexibility of use and long-lasting operation [9–11], a considerable effort has been devoted to the area of self-powered sensors over the past few years.

Ionic conductive gel is a class of three-dimensional crosslinked "soft and wet'' materials containing free ions [12–15], which is widely applied in adhesives [16,17], energy harvesters and storage devices [18,19], ionic skin [20,21], touch panel [22,23], bioelectronics [24] and so on. Especially, their exceptional properties in softness, versatility, electrical conductivity, iontronics and responsiveness render them as a promising candidate in the fabrication of the new-generation flexible sensor and energy harvesters [25–30]. Therefore, ionic conductive gels become the most potential and competitive self-powered sensing materials, which pave the way for the development of self-powered sensors [31]. For example, some self-powered stress sensors that generate electricity in response to mechanical deformation have been successfully developed by employing the ionic conductive gels as force-responsive electrodes, including triboelectric gel sensors [32,33], piezoelectric gel sensors [34,35] and ionic diode gel sensor [36,37] based on triboelectric effect, piezoelectric effect and thickness-dependent self-induced potential effect. In addition to mechanoelectric conversion mechanism, more self-powered mechanism have also been proposed to meet the diversified demands of environment sensing, such as thermoelectric [38], magnetoelectric [39], hydrovoltaicenergy conversion mechanism [40], which can efficiently harvest various sources of energy (i.e., thermal, magnetic, chemical energy, etc.) and convert them into electrical energy. For instance, Zhang's group have developed a series of thermoelectric gel based self-powered sensing devices utilizing various polymer networks and redox pairs, and realizing the real-time monitoring for ambient temperature, body temperature and even breath [41,42].

* Corresponding authors at: Key Laboratory of Marine Materials and Related Technologies, Zhejiang Key Laboratory of Marine Materials and Protective Technologies, Ningbo Institute of Material Technology and Engineering, Chinese Academy of Sciences, Ningbo 315201, China.
E-mail addresses: weijunjie@nimte.ac.cn (J. Wei), tao.chen@nimte.ac.cn (T. Chen).

https://doi.org/10.1016/j.cej.2024.149836
Received 12 December 2023; Received in revised form 26 January 2024; Accepted 18 February 2024
Available online 19 February 2024

Although ionic conductive gel based self-powered sensors have been able to realize the perception of various signals, the types of these perceptable signals are still very few, which also limits their multi-scene applications.

Sunlight-intensity sensing technology is of great significance for the fields of intelligent lighting, smart agriculture, energy conservation in building and so on [43,44]. Recently, Some photo-driven self-powered sensing devices have been developed by ingenious structure [45–47]. Unfortunately, it is still challenging to endow ionic conductive gels with intrinsic self-powered sunlight-intensity sensing function, because traditional ionic conductive gels lack the ability to convert solar energy directly into electricity. Recently, with the assistance of photothermal electrodes, researchers have fabricated thermoelectric gel devices that can use solar power to generate electricity [48,49], so that the sunlight intensity can be sensed to a certain extent. However, this non-integrated function structure, the separation between photothermal component and thermoelectric component, will cause excess energy loss in the conversion and conduction processes, reducing the utilization efficiency of solar energy and sensing performance. Therefore, it is a challenging and rewarding to design the "all-in-one" photosensitive gels to achieve self-powered sunlight-intensity sensing.

Herein, a photosensitive Janus ionogel with pseudo-photoelectric cascade conversion was developed by utilizing the synergism of photothermal effect and thermoelectric effect. The conductive carbon black was introduced to the ionogels to construct the Janus ionogels, which was able to convert solar energy to heat then to electricity. The photosensitive Janus ionogels have excellent thermoelectric properties, including high Seebeck coefficient of 19.5 $mV{\cdot}K^{-1}$ and ZT value of 0.63. The photosensitive Janus ionogels can realize the solar energy harvesting and sensing of sunlight intensity which can be applied to construct a smart electrochromic device by coupling this self-powered sensor device with an electrochromic device.

2. Experimental section

2.1. Material

1-ethyl-3-methylimidazolium dicyanamide (98 %, EMIM:DCA), sodium dicyanamide (96 %, Na:DCA), N,N-Dimethylallylamine (98 %, DMAA), 2, 2-azobisisobutyronitrile (AIBN), 2,2-Diethoxyacetophenone (>95 %, DEAP), polypyrrole (PPy), graphene oxide (GO) were purchased from Aladdin Industrial Co., N,N'-Methylenebisacrylamide (90 %, MBAA) was purchased from Macklin. Conductive carbon black (super-P) was purchased from Alfa Aesar. Carbon nanotubes (CNTs) and carboxyl-modified carbon nanotubes (CNTs-COOH) were purchased from Chengdu Organic Chemicals Co. Ltd. Cuttlefish juice was purchased from Qingdao Risheng Chang Food Ingredients Co. Ltd. ITO electrodes were purchased from Luoyang Shangzhuo Technology Co. Ltd. All materials were used without further purification.

2.2. Synthesis of photosensitive Janus ionogels

Typically, the photosensitive Janus ionogel was prepared by the following method: Firstly, 1012.5 mg EMIM:DCA, 16.2 mg Na:DCA, 337.5 mg DMAA and 3.4 mg MBAA were mixed to form original solution. Secondly, pre-polymerization solution A was configured by adding 1.1 mg conductive carbon black and 0.5 mg thermal initiator AIBN into the above solution, then a thermoelectric ionogel layer with photothermal function was obtained through thermal polymerization at 90 °C for 30 min. Other photothermal gels are prepared with the same mass of photothermal material as that of conductive carbon black. Thirdly, a pre-polymerization solution B containing 2.8 mg photoinitiator DEAP was configured through the similar method, but replacing conductive carbon black and AIBN with DEAP. Finally, the pre-polymerization solution B was injected into the reaction mold assembled from quartz glass and thermoelectric ionogel, and the photosensitive Janus ionogel containing photothermal ionogel layer and thermoelectric ionogel layer was successfully prepared through placing the reaction mold under ultraviolet radiation (20 W, 365 nm), namely, the in-situ polymerization of photothermal gel on a thermoelectric gel layer.

2.3. Measurement of Seebeck coefficient

The Seebeck coefficients are measured using a system developed in-house, at the room temperature of 30 ℃. Electrochemical station (CHI660E, CH Instruments Ins.) and temperature control module (TCM-M207, Chengdu Yexian Technology Co., LTD) were employed to measure the voltage and temperature, respectively.

2.4. COMSOL simulation

The light-thermal conversion and heat conduction were simulated by COMSOL Multiphysics software. The photosensitive Janus ionogels (15 × 15 × 6 mm) model includes 1 mm photothermal ionogel and 5 mm thermoelectric ionogel. The basic physical properties of the photosensitive Janus ionogel were determined according to the results of previous experiments. The initial temperature was 30 °C, the solar intensity was 1000 W m^{-2}, and the angle of incidence was 90°.

2.5. Analysis of light-thermal-electrical conversion

The light-thermal-electrical cascade conversion performance was studied by monitoring the thermal voltages of photosensitive Janus ionogel based device exposuring to simulated sunlight (Princesse PL-X300DF), using electrochemical station CHI660E. Two ITO electrodes were used as electrodes and the wires were fixed to the ITO electrodes with conductive silver paste. Infrared images were taken using an optris PI400. The temperature difference between the same vertical surfaces at the outer surface of the photosensitive Janus ionogel was chosen as the temperature difference between the two sides of the photosensitive Janus ionogel.

The energy density (E) harvested during the stage II can be calculated with regard to this equation, $E=\frac{\int U^2/Rdt}{V}$, where U, R and V are the voltage on the external load, the external resistance and the volumes of the device, respectively.

2.6. Characterizations

The thermal conductivity was measured using Hotdisk TPS 3500.

The ionic conductivity was measured by AC impedance spectra using electrochemical station CHI660E, in the frequency range of 0.1 Hz to 100 kHz. The intersection of the curve at the real part was taken as the bulk resistance of the ionogel (R), and the ionic conductivity of the sample was calculated according to the following equation:

$$\sigma = \frac{d}{RS}$$

where d is the thickness of the thermoelectric ionogel and S is the electrode area. Thermoelectric ionogel sample (20 mm × 20 mm × 4 mm) was sandwiched between two stainless steel electrodes (40 mm × 20 mm).

Thermogravimetric analysis was used to measure the thermal decomposition temperature of the ionogels, the heating interval was 20 °C ~ 500 °C, and the heating rate was 5 °C/min.

The morphology structure was characterized using SEM technique (Hitachi S4800).

The absorption of the ionogels was measured using Lambda 950 UV–vis-NIR spectrophotometer in the range of 250 ~ 2500 nm.

The peeling strength was measured using a universal tensile machine (Zwick Z1.0) with tensile speed of 50 $mm{\cdot}min^{-1}$.

3. Results and discussion

3.1. Design and construction of the photosensitive Janus ionogel

As shown in Fig. 1**a**, the photosensitive Janus ionogel is comprised of a photothermal ionogel layer and thermoelectric ionogel layer. Owing to photothermal effect, the upper photothermal ionogel layer containing of conductive carbon black can effectively convert light energy into heat energy (Fig. 1b), which is then converted into electric energy by the generated temperature gradient and thermoelectric effect of the underlying ionogel layer (Fig. 1c). Based on this, a self-powered sunlight-intensity sensing device is fabricated by this photosensitive Janus ionogel and indium tin oxid (ITO) electrodes (Fig. 1d). Thanks to the high light transmittance of the ITO electrode, the sunlight can penetrate the ITO electrode and radiate on the photosensitive ionogel, so as to finally achieve the light intensity-dependent electric signal through "light-thermal-electric" cascade conversion. This ionotronic based on photosensitive Janus ionogel can not only apply to harvest solar energy acting as solar cell, but also play as an intelligent switch for electrochromic glazing using the self-powered sensing capacity, which is conducive to smarter and more efficient building energy conservation (Fig. 1e). The photosensitive Janus ionogel shows broad prospects in the field of solar energy harvesting and sensing.

The photosensitive Janus ionogel consists of photothermal ionogel layer and thermoelectric ionogel layer, which are prepared by the following steps. Firstly, a certain amount of monomer N,N-Dimethylallylamine (DMAA), crosslinking agent N,N'-Methylenebisacrylamide (MBAA) and doped sodium salt sodium dicyanamide (Na:DCA) were dissolved in the ionic liquid 1-ethyl-3-methylimidazolium dicyanamide (EMIM:DCA) under stirring, and a transparent and homogeneous original solution was prepared (Fig. 2**a**). In order to obtain a photothermal ionogel with photothermal conversion performance, conductive carbon black and 2, 2-azobisisobutyronitrile (AIBN) were introduced into the above original solution as photothermal dopants and thermal initiator, forming pre-polymerization solution A. After thermal initiation at 90 °C for 30 min, a photothermal ionogel film was polymerized (Fig. 2b). Afterwards, a pre-polymerization solution B was configurated through adding photoinitiator 2,2-Diethoxyacetophenone (DEAP) into original solution, and the photothermal ionogel film was prepared by in-situ photo-polymerization on the upper surface of photothermal ionogel film (Fig. 2c). Based on the network interpenetration during in-situ polymerization, a photosensitive Janus ionogel with strong interfacial binding was successfully obtained by the above two step polymerization method (Fig. 2d).

To study the interface properties between the two ionogel layers, the interfacial structure of photosensitive Janus ionogel was observed by a polarizing microscopy. As shown in Fig. S1, the two ionogel films were bonded tightly, and there was no obvious interfacial gap at the interface of two ionogel layers. Besides, scanning electron microscopy (SEM) was used to observe the microstructure of ionogel interface. As shown in Fig. 2e, the SEM image clearly shows the microstructure of the cross section. Due to the small size (~40 nm) of conductive carbon black particles, they can be uniformly filled into the porous structure of photothermal ionogel (Fig. S2), leading to obvious differences in the microstructure of photothermal ionogel film and thermoelectric ionogel film. Consistent with the results of optical observation, there is no apparent gap in the interfacial microstructure between the upper and lower ionogel layers, which proves the conformal contact between the two ionogels again. This "all-in-one" structure is mainly attributed to the in-situ polymerization of thermoelectric ionogel. In the in-situ polymerization process, the monomers within pre-polymerization solution B will diffuse into the network structure of the photothermal ionogel driven by the concentration gradient, thus forming a network interpenetrating structure at the interface after polymerization. As a result, there is a strong binding force between the photothermal ionogel layer and thermoelectric ionogel layer, which was verified by the interfacial peeling test of the photosensitive Janus ionogel. As depicted in Fig. 2f, the interfacial peeling strength between the two ionogels reached about

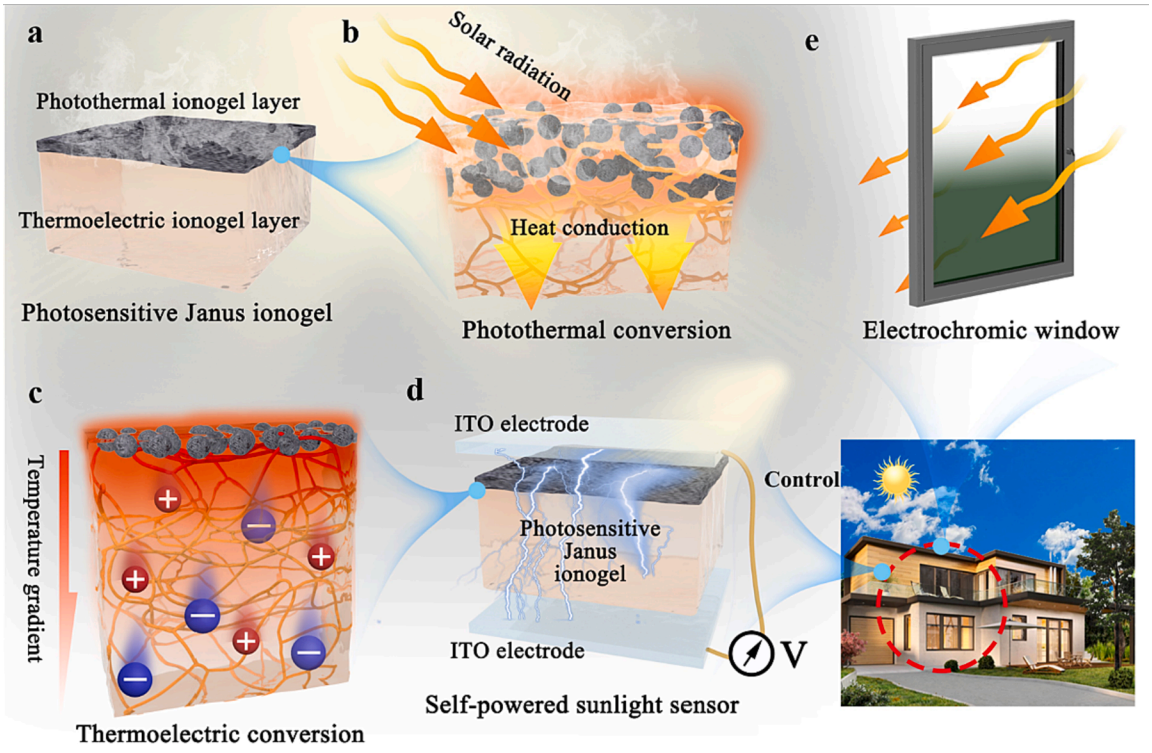

Fig. 1. Structure and application of the photosensitive Janus ionogel based self-powered sensing device. (a) Structure of photosensitive Janus ionogel. (b) Photothermal conversion process of upper photothermal ionogel layer; (c) Thermoelectric conversion process of underlying ionogel layer. (d) Structure of self-powered solar-intensity sensing device. (e) Application in automatic color adjustment of the smart windows by playing as sunlight-sensing voltage switch.

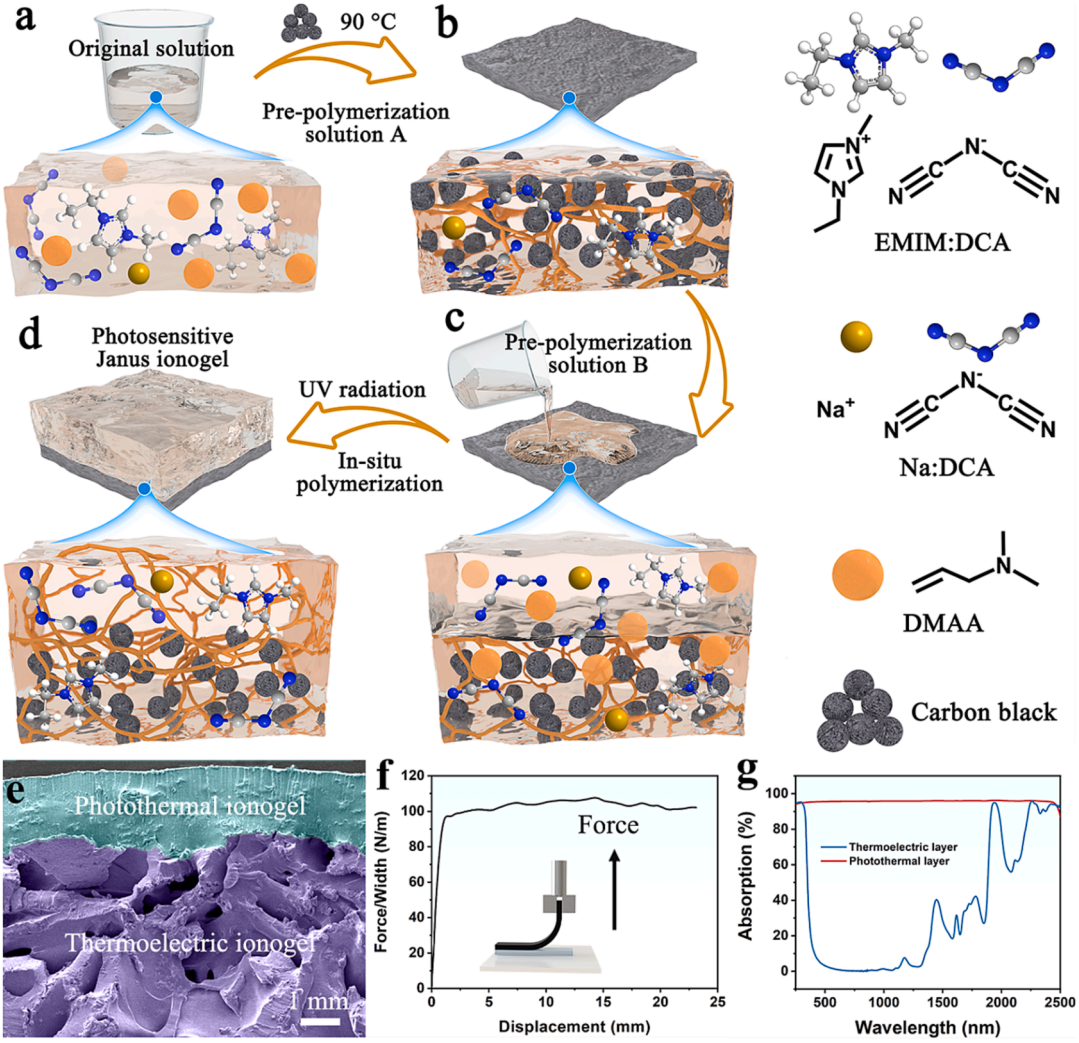

Fig. 2. Fabrication and characterization of photosensitive Janus ionogel. (a) Original solution. (b) Photothermal ionogel. (c) In-situ photo-polymerization of thermoelectric ionogel. (d) Photosensitive Janus ionogel. (e) SEM image of the cross section of photosensitive Janus ionogel. (f) Interfacial peeling test of photosensitive Janus ionogel. (g) UV–vis-NIR absorption spectra of photothermal ionogel and thermoelectric ionogel.

100 $N{\cdot}m^{-1}$, confirming the thermoelectric ionogel film was firmly bonded with photothermal ionogel film.

Considering the high operating temperature of the photosensitive Janus ionogel resulted from high-temperature environment or photothermal effect, the thermal stability of the ionogels was characterized by thermogravimetric analysis (TGA). As shown in Fig. S3, both photothermal ionogel and thermoelectric ionogel were found to be thermally stable in the temperature range of 25 °C to 250 °C.

UV–vis-NIR absorption spectra were used to investigate the optical properties of the photosensitive Janus ionogel. As shown in Fig. 2g, compared to the low solar light absorption (~5%) of the thermoelectric ionogel without conductive carbon black, the photothermal ionogel loaded with a large amount of conductive carbon black exhibited a high solar absorption in the whole range of light wavelength (250 ~ 2500 nm), even exceeded 95 % in the wavelength range of 300 ~ 2400 nm, thereby suggesting that the doping of conductive carbon black has significantly improved the solar light absorption ability. This high absorption capacity for sunlight provides the energy base for the generation of thermal energy through photothermal conversion.

3.2. Photothermal and thermoelectric properties of photosensitive Janus ionogel

Good photothermal properties were a prerequisite for achieving the "light-thermal-electric" cascade conversion of photosensitive Janus ionogel. As shown in Fig. S4, the photothermal ionogel with conductive carbon black exhibited excellent photothermal conversion performance due to the good dispersion, compatibility and photothermal ability. Of course, in addition to conductive carbon black, other photothermal materials (such as carbon nanotubes, CNTs; carboxyl-modified carbon nanotubes, CNTs-COOH; cuttlefish juice; polypyrrole, PPy; graphene oxide, GO) can also endow ionogel with photothermal properties.

A higher light-induced heating rate and equilibrium temperature under solar radiation are conducive to form a larger temperature difference and temperature gradient at both ends of the photosensitive Janus ionogel. Therefore, the conductive carbon black content in the photothermal ionogel and the thickness of ionogel were further optimized. The photothermal properties of the ionogels with different loadings of conductive carbon black are shown in Fig. 3**a**, where higher heating rates and equilibrium temperatures were obtained at a higher content of conductive carbon black when the content is below 5 $mg{\cdot}mL^{-1}$. However, the further increase of content has no obvious effect on the change of light-induced temperature, and thus the content of

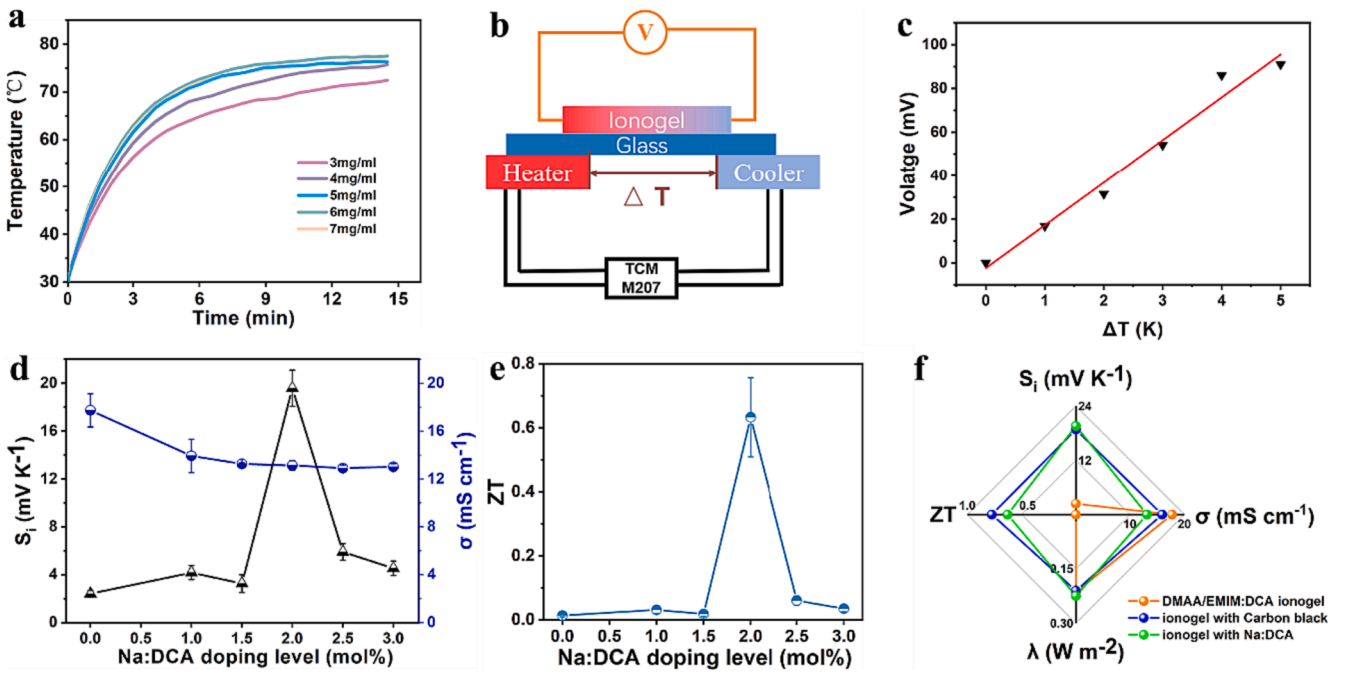

Fig. 3. Photothermal and thermoelectric properties of photosensitive Janus ionogel. (a) Photothermal properties of photothermal ionogels with different conductive carbon black content. (b) Structure of ionic Seebeck coefficient test configuration. (c) Seebeck coefficients of thermoelectric ionogel obtained from the V-ΔT relationship curve. (d) Ionic Seebeck coefficients and conductivity of thermoelectric ionogels with various Na:DCA doping level. (e) ZT value of thermoelectric ionogels with various Na:DCA doping level. (f) Comparison of thermoelectric properties of three ionogels, including thermoelectric ionogel without Na:DCA, ionogel with conductive carbon black (i.e. photothermal ionogel), and thermoelectric ionogel with 2.0 mol% Na:DCA.

conductive carbon black is determined to be 5 mg·mL^{-1}. The relationship between the thickness of photothermal ionogel and the photothermal properties of ionogel were shown in Fig. S5. Thinner photothermal ionogels had a better heating rate, but cannot produced higher temperatures due to their smaller size and limited ability to absorb sunlight. Photothermal ionogels that are too thick can only absorb a limited amount of energy and produce a limited temperature. A highest equilibrium temperature of 67.2 °C and a faster heating rate were achieved when the thickness reached 1 mm.

Ionic Seebeck coefficient (S_i) is one of the key parameters that determine the energy conversion efficiency of ionic thermoelectric materials, according to the definition of the thermal power Figure of merit (ZT). As illustrated in Fig. 3b, the ionic Seebeck coefficients were measured using the homemade configuration along in-plane direction, and the temperature difference (ΔT) and voltage difference (ΔV) between the two terminals (hot terminal and cold terminal) of the ionogels were recorded. The effect of monomer content on S_i of ionogel was studied firstly. The ionic Seebeck coefficient of the pristine DMAA ionogel without sodium salt Na: DCA increased with the increasing content of DMAA until 75 wt%, which was due to the increasing interaction between DMAA and EMIM:DCA enhancing the difference in the mobilities of anions and cations. However, increasing blocking effect of denser polymer network on ionic migration, which limited the further increasing of the ionic Seebeck coefficient. As shown in Fig. S6, a maximum S_i value was 2.44 mV·K^{-1} at 75 wt% EMIM:DCA. The ionic conductivities, another important parameter of thermoelectric performance, of the ionogels were measured by the AC impedance spectroscopy. As shown in Fig. S7, the ionic conductivity of pristine DMAA ionogels without Na:DCA decreased with decreasing IL content due to the increasing blocking effect of denser polymer network on ionic migration.

According to the research achievement reported previously [50], the addition of another anions or cations to ionogels may be influence the interaction of the origin anions and cations, which is able to improve the thermoelectric performance of ionogels by increasing the difference in the mobilities of anions and cations. Based on this proposed theory, cationic dopant Na:DCA was introduced into the ionogels expecting to improve the thermoelectric properties of the ionogels. Considering that the ionogel possesses the highest S_i value when the EMIM:DCA content is 75 wt%, the following cationic doping tests were performed on ionogels with an EMIM:DCA content of 75 wt%. The ionic Seebeck coefficient and ionic conductivity of Na:DCA-doping ionogels are shown in Fig. 3d. The addition of Na:DCA dramatically changed the ionic thermoelectric properties of ionogels due to the interactions between the doped Na^+ and DCA^-, and the S_i value reached a maximum value of 19.5 mV·K^{-1} at a Na:DCA doping content of 2.0 mol%. It is worth noting that the ionic conductivity of the ionogel is negatively correlated with the amount of doping Na:DCA. As the doping amount of Na:DCA gradually increased to 3.0 mol%, the ionic conductivity monotonically decreases from 17.7 mS·cm^{-1} to 13 mS·cm^{-1}. This result is due to the fact that the doping of Na^+ ions will increase the viscosity of EMIM:DCA and reduce the ion migration rate. Besides, the doping of Na:DCA had no significant effect on the thermal conductivity, another key property affecting thermoelectric performance, of the ionogel (Fig. S8). The thermal power index ZT that reflecting the energy conversion efficiency also affected by the doping content of Na:DCA. As shown in Fig. 3e, the ZT value reaches a maximum of 0.63 at the optimum Na:DCA doping level of 2.0 mol%. However, because both ionic Seebeck coefficient and ionic conductivity decreased with increasing Na:DCA doping at high Na^+ doping level, the ZT value also decreased with further increasing Na:DCA doping. As shown in Table S1, compared to other thermoelectric ionogels, the thermoelectric properties of this photosensitive Janus ionogel had good thermoelectric property.

As an important part of photosensitive Janus ionogel, the thermal power of photothermal ionogel layer will affect the overall thermoelectric conversion ability of the Janus ionogel. Therefore, the thermoelectric properties of the photothermal ionogel layer doped with conductive carbon black was also investigated. As shown in Fig. 3f, the thermoelectric properties of three kinds of ionogels, including pristine thermoelectric ionogel without Na:DCA, photothermal ionogel, and

thermoelectric ionogel with Na:DCA, were compared comprehensively. Obviously, the introduction of Na:DCA greatly improved the thermoelectric properties of ionogels, but the introduction of conductive carbon black imparted photothermal properties to the ionogel without significantly reducing its thermoelectric properties.

3.3. Pseudo-photoelectric performance of photosensitive Janus ionogel based capacitor

Inspired by the good photothermal performance and thermoelectric performance of the photosensitive Janus ionogel, a self-powered sensing capacitor with solar energy harvesting capacity were fabricated by assembling photosensitive Janus ionogel and ITO electrodes as current collectors. The self-powered sensing capacitor can generate voltage through a cascade mechanism of "light-thermal-electric" conversion. As a verification, a photothermal catalytic device (Precise PL-X300DF) was used to simulate sunlight, and the voltage changes of the device were recorded using a CHI660E electrochemical workstation. As shown in Fig. 4**a** and Fig. S9, when simulated solar illumination was applied to the photothermal ionogel layer of the self-powered device, a decreasing temperature gradient from top to bottom occurred within the photosensitive Janus ionogel due to the photothermal effect and heat conduction, which was also consistent with the simulation results (Fig. 4b). Meanwhile, this temperature gradient lead to the differential migration of cations and anions from the illuminated side (hot terminal) to the non-illuminated side (cold terminal). As a result, an asymmetric ion concentration aggregation and distribution appeared on two sides of photosensitive Janus ionogel, thereby generating an obvious voltage on two electrodes due to the induction of charges by ions (Stage I). In stage II, the device was connected to an external load. To balance the anions and cations on the two electrodes, a current was generated in the closed circuit and the voltage across the external load was reduced. In stage III, the light source was turned off and the circuit was disconnected, and the voltage between the two electrodes dropped to a negative value due to the generation of holes and electrons on each side of the electrodes as a result of the current generation in stage II. In the stage IV, the circuit was re-connected, and the electrons and holes accumulated in both electrodes returned to the initial conductive state, generating a current opposite to that of the second stage, and the voltage between the two electrodes gradually decreased to zero. This excellent photoresponsive thermoelectric performance not only enables the ionogel capacitor with thermal energy harvesting capability, just like traditional thermoelectric materials, but also gives the additional solar energy harvesting capability and self-powered light sensing function.

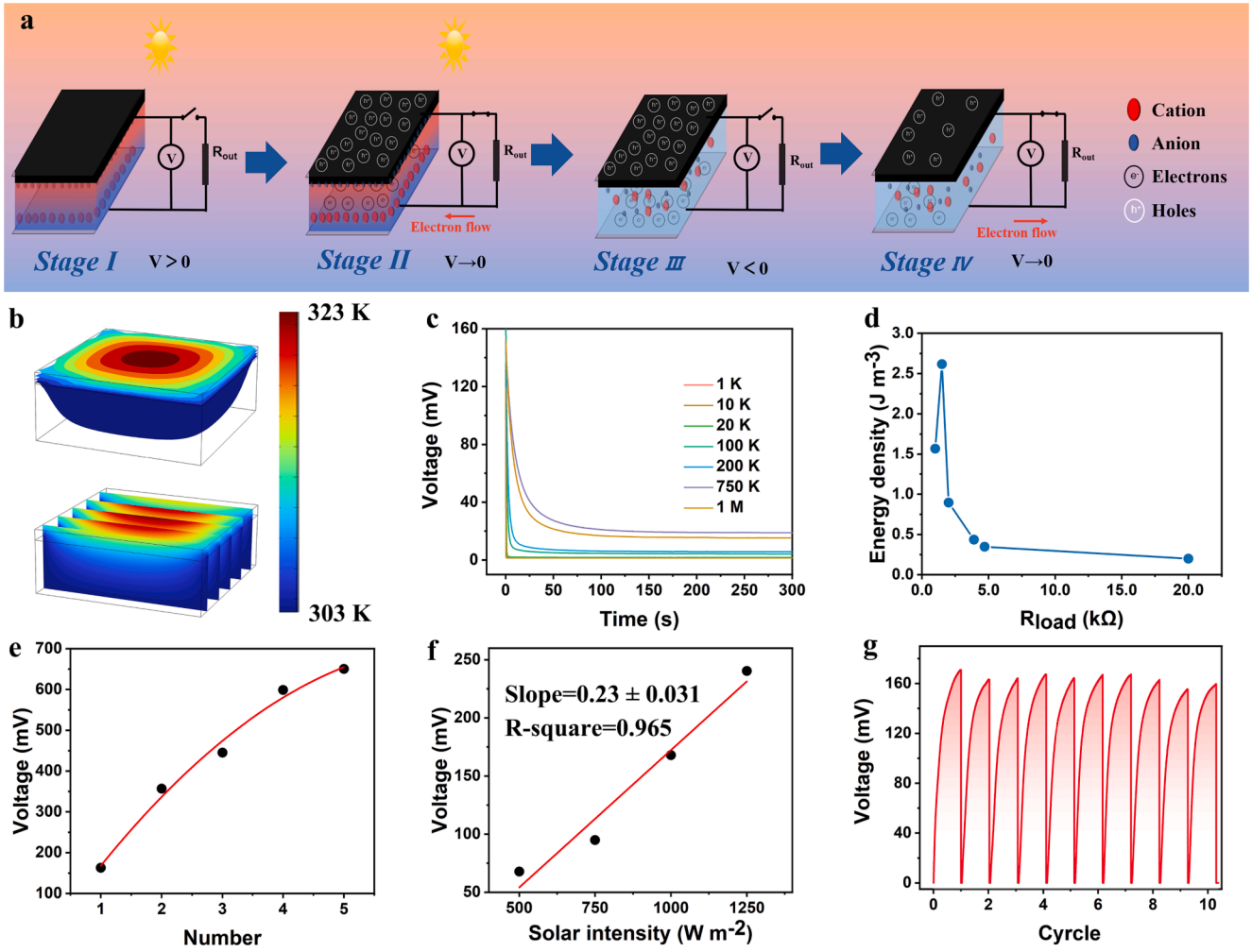

Fig. 4. "Light-thermal-electric" cascade conversion performance of photosensitive Janus ionogel based capacitor. (a) Schematic illustration of the work principles of photosensitive Janus ionogel based capacitor in four stages. (b) Temperature distribution for the photosensitive Janus ionogel from COMSOL simulation. (c) Output voltage decay curves on an external load with different resistances during stage II. (d) The total energy density during stages II on the different resistance of the external load. (e) Output voltage of photosensitive Janus ionogel based capacitor formed by different number in series. (f) Thermalvoltage of photosensitive Janus ionogel under different sunlight intensities. (g) Cyclic sensing performance of photosensitive Janus ionogel based self-powered sensor under sunlight intensity of 1000 W·m^{-2}.

As a solar energy harvesting device, energy density, which can be deduced from the discharge curve at stage II, is an important index to evaluate its performance. As shown in Fig. 4c, due to the intrinsic capacitive feature, the ionic thermovoltage of ionic device decays and then reaches a relatively low output voltage during stage II, Interestingly, the ionic thermovoltage becomes lower for higher external resistances due to the increase in the decay time constant, which is defined as $\tau = R{\cdot}C$, where R and C are the external resistance and capacitance, respectively. The energy harvested in a light-thermal-electric cycle is related to the external load. The volume energy density of the device during stage II was calculated according to the equation $E=\frac{\int U^2/Rdt}{V}$. The average power density of the device was calculated in terms of the equation, $P=\frac{E}{t}$, where E and t were the volume energy density of the device during stage II and the time of the device discharge, respectively. As shown in Fig. 4d, the volume maximum energy density reached 2.6 $J{\cdot}m^{-3}$ at an external load of 1500 Ω, and the power density was 2.8 $W{\cdot}m^{-3}$, suggesting the good solar energy harvesting capability. Although its energy density is lower than traditional solar cells due to the multi-stage energy conversion and loss, the ionic device based on a brand-new solar energy harvesting mechanism of "light-thermal-electric" cascade conversion also provides a new candidate in the field of solar energy harvesting.

In order to adapt to the different voltages required in different environments, it is important for photosensitive Janus ionogel based capacitor to be able to be connected in series. As shown in Fig. S10, several capacitors were connected in series and their output voltages were measured under a simulated solar intensity of 1000 $W{\cdot}m^{-2}$. As shown in Fig. 4e, the total voltage was almost linearly related to the number of series connections. Note here that due to the limited irradiation area of the simulated sunlight used in the test and the light-intensity attenuation at the edge, the relationship between the total voltage and the number of series connections gradually deviated from a straight line. This quantity-dependent thermovoltage provides the possibility for powering the electrical devices that need high operating voltage.

Since the thermovoltage of photosensitive Janus ionogel based capacitor is proportional to the temperature difference between the two terminals, and the temperature difference is related to the intensity of sunlight, there is also a corresponding relationship between the thermovoltage and the intensity of sunlight, that is, the self-powered light intensity perception. In order to verify the potential application of the device for light intensity sensing, the thermovoltage of the device under different light intensities were tested (Fig. S11). As shown in Fig. 4f, the prepared devices were able to generate different voltages for different sunlight intensities, confirming their potential application in sunlight intensity sensing as sensor. Excellent cycling performance is an important indicator for evaluating self-powered sensing devices. The cycling performance of the device was studied under a simulated sunlight intensity of 1000 $W{\cdot}m^{-2}$. As shown in Fig. 4g, the voltage generated by the device was maintained at about 165 mV for 10 time cycles, proving its good cycling performance and feasibility for long-term operation.

3.4. Application of self-powered sunlight sensor

Using the synergism of photothermal effect and thermoelectric effects, the self-powered sensor based on photosensitive Janus ionogel can generate voltage under sun. Fig. 5**a** showed the variation of sunlight intensity and voltage of the self-powered device under cloudy weather. Changes in the sunlight intensity falling on the self-powered sensor device were the main cause of the detected voltage changes. The voltage of self-powered sensor increased when there is no cloud and decreased when the sun is obscured by clouds synchronously. The good consistency of voltage change and sunlight intensity change confirms the sensitivity of the self-powered sensor to sunlight intensity. Fig. 5b

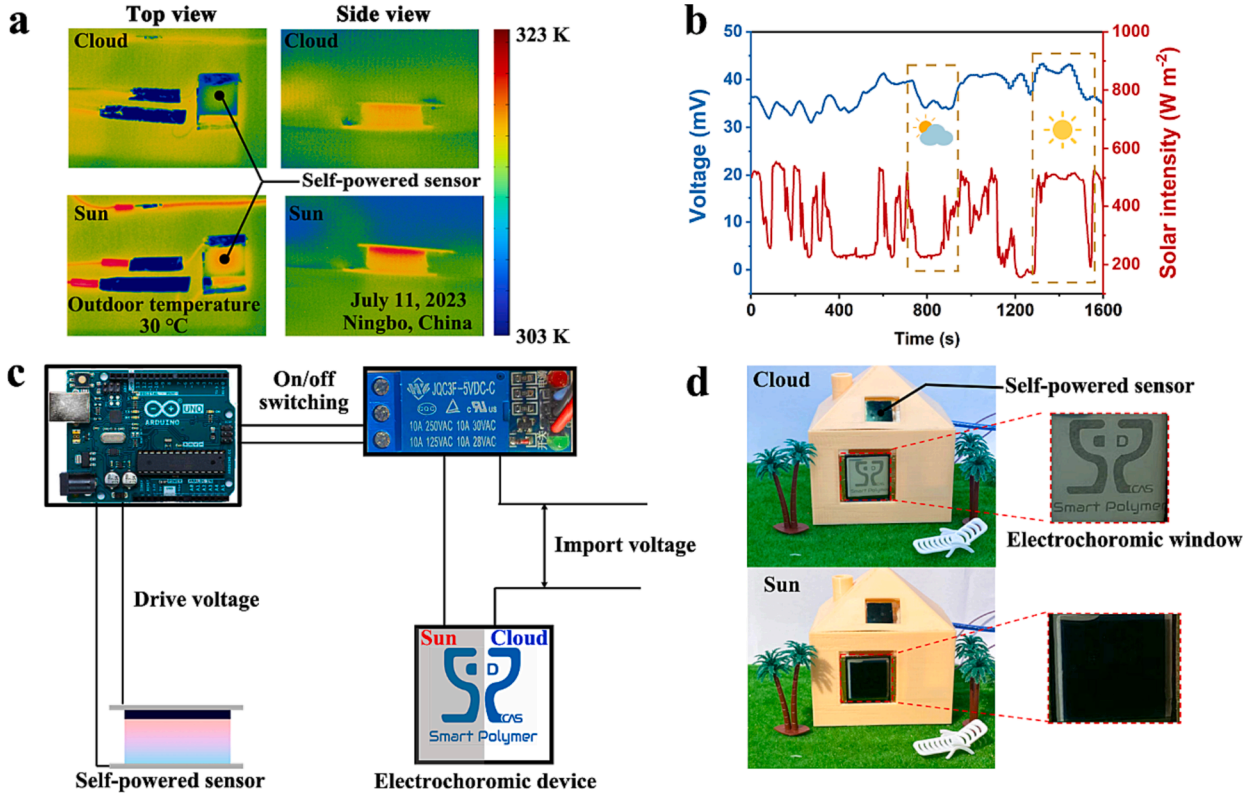

Fig. 5. Application of photosensitive Janus ionogel based self-powered sunlight sensor. (a) Infrared images of the top and side views of the device on sunny and cloudy days. (b) Variation of sunlight intensity and voltage of the self-powered device under cloudy weather. (c) Components of the self-powered sensor. (d) Application of self-powered sensor coupled with electrochromic device.

showed the infrared images of the top and side of the device on sunny and cloudy days. Under different light intensities, the ionogel exhibited a vertical temperature distribution with different temperature differences, which in turn generate different voltages.

To demonstrate the practicability of self-powered sensor for sunlight intensity detection, we constructed a smart electrochromic device by coupling this self-powered sensor with an electrochromic device (Fig. 5c). Through setting a suitable threshold voltage that matches the thermovoltage at high sunlight intensity, the self-powered sunlight sensor can be used as an intelligent voltage switch to control the electrochromic behavior of smart Window, so as to realize the automatic color adjustment of the smart windows adapted to the sunlight intensity. As shown in Fig. 5d, when the sunlight intensity is high on a sunny day, the self-powered sensor outputted a high thermovoltage that is higher than threshold value, and the smart electrochromic glass showed a dark color. On the contrary, the thermovoltage correspondingly quickly dropped below the threshold when the sunlight intensity decreased, thereby controlling the color of electrochromic glass from dark to light, allowing more sunlight to enter the room through the glass window. This scene fully demonstrates the potential of the photosensitive Janus ionogel based sensor in the field of sunlight sensing and energy conservation in building. In fact, if the energy density of the device can be further improved in the later research, such as introducing the thermogalvanic effect based on redox couple, the photosensitive Janus ionogel based device is expected to provide energy supply for the smart window on the basis of self-powered sensing, so that the smart window can get rid of the dependence on external power.

4. Conclusion

In this study, a photosensitive Janus ionogel containing photothermal layer and thermoelectric layer was proposed by in-situ polymerization of thermoelectric ionogel on the photothermal ionogel film. The photosensitive Janus ionogel not only possesses excellent thermoelectric performance, including high Seebeck coefficient of 19.5 $mV{\cdot}k^{-1}$ and ZT value of 0.63, but also can spontaneously form a temperature gradient under sunlight due to the prominent photothermal effect of the upper layer, i.e., pseudo-photoelectric effect. Utilizing the synergism of photothermal effect and thermoelectric effect, the photosensitive Janus ionogel can convert solar energy into electric energy by the "light-thermal-electric" cascade conversion, and the capacitor based on this photosensitive Janus ionogel exhibits a maximum volume energy density of 2.6 $J{\cdot}m^{-3}$ through harvesting solar energy. Furthermore, the sunlight-dependent thermovoltage endows the photosensitive Janus ionogel based device with self-powered sensing ability to sunlight intensity. As a validation, the self-powered sensor successfully realizes the sensitive perception for sunlight intensity and the intelligent control for electrochromic window. This photosensitive Janus ionogel provides a new material candidate for solar energy utilization and light sensing. In the future, the self-powered capability and sensing performance of this photosensitive Janus ionogel is expected to be further improved by thermoelectric performance optimization, and it is supposed to be applied in the field of flexible optoelectronics, such as photoelectric fire detector and human-like visual perception.

Declaration of competing interest

The authors declare no competing financial interests.

CRediT authorship contribution statement

Jiale Sun: Writing – original draft, Visualization, Investigation. **Yanan Liu:** Investigation. **Junjie Wei:** Writing – review & editing, Supervision, Funding acquisition, Conceptualization. **Peng Wei:** Writing – review & editing. **Tao Chen:** Writing – review & editing, Supervision, Project administration.

Declaration of competing interest

The authors declare that they have no known competing financial interests or personal relationships that could have appeared to influence the work reported in this paper.

Data availability

Data will be made available on request.

Acknowledgements

This work was supported by the National Natural Science Foundation of China (52103152), Ningbo Key R&D Program (2023Z089), Ningbo Natural Science Foundation (2022J286).

Appendix A. Supplementary data

Supplementary data to this article can be found online at https://doi.org/10.1016/j.cej.2024.149836.

References

[1] A. Alagumalai, W. Shou, O. Mahian, M. Aghbashlo, M. Tabatabaei, S. Wongwises, Y. Liu, J. Zhan, A. Torralba, J. Chen, Z. Wang, W. Matusik, Self-powered sensing systems with learning capability, Joule 6 (2022) 1475–1500, https://doi.org/10.1016/j.joule.2022.06.001.
[2] M. Du, X. Chen, K. Zhang, Origins of enhanced thermoelectric transport in free-standing PEDOT nanowires film modulated with ionic liquid, ACS Appl. Energy Mater. 4 (2021) 4070–4080, https://doi.org/10.1021/acsaem.1c00422.
[3] Z. Huo, Y. Wei, Y. Wang, Z.L. Wang, Q. Sun, Integrated Self-Powered Sensors Based on 2D Material Devices, Adv. Funct. Mater. 32 (2022) 2206900, https:// doi.org/10.1002/adfm.202206900.
[4] B. Zhou, J. Liu, X. Huang, X. Qiu, X. Yang, H. Shao, C. Tang, X. Zhang, Mechanoluminescent-Triboelectric Bimodal Sensors for Self-Powered Sensing and Intelligent Control, Nano-Micro Lett. 15 (2023) 72. https://link.springer.com/10.1007/s40820-023-01054-0.
[5] S. Liu, M. Zhang, J. Kong, H. Li, C. He, Flexible, durable, green thermoelectric composite fabrics for textile-based wearable energy harvesting and self-powered sensing, Compos. Sci. Technol. 243 (2023) 110245, https://doi.org/10.1016/j.compscitech.2023.110245.
[6] P.J. Taroni, G. Santagiuliana, K. Wan, P. Calado, M. Qiu, H. Zhang, N.M. Pugno, M. Palma, N. Stingelin-Stutzman, M. Heeney, O. Fenwick, M. Baxendale, E. Bilotti, Toward Stretchable Self-Powered Sensors Based on the Thermoelectric Response of PEDOT:PSS/Polyurethane Blends, Adv. Funct. Mater. 28 (2017) 1704285, https://doi.org/10.1002/adfm.201704285.
[7] L. Zhang, R. Fang, X. Li, C. Tian, J. Li, X. Cui, H. Zhang, Self-powered physiological monitoring strategy enabled by adaptive dual-network thermogalvanic hydrogels, Sens. Actuators A: Phys. 361 (2023) 114604, https://doi.org/10.1016/j.sna.2023.114604.
[8] Y. Feng, J. Yu, D. Sun, C. Dang, W. Ren, C. Shao, R. Sun, Extreme environment-adaptable and fast self-healable eutectogel triboelectric nanogenerator for energy harvesting and self-powered sensing, Nano Energy 98 (2022) 107284, https://doi.org/10.1016/j.nanoen.2022.107284.
[9] J. Li, Z. Wang, S.A. Khan, N. Li, Z. Huang, H. Zhang, Self-powered information conversion based on thermogalvanic hydrogel with interpenetrating networks for nursing aphasic patients, Nano Energy 113 (2023) 108612, https://doi.org/10.1016/j.nanoen.2023.108612.
[10] X. Li, J. Li, T. Wang, S.A. Khan, Z. Yuan, Y. Yin, H. Zhang, Self-Powered Respiratory Monitoring Strategy Based on Adaptive Dual-Network Thermogalvanic Hydrogels, ACS Appl. Mater. Interfaces 14 (2022) 48743–48751, https://doi.org/10.1021/acsami.2c14239.
[11] R. Fu, L. Tu, Y. Zhou, L. Fan, F. Zhang, Z. Wang, J. Xing, D. Chen, C. Deng, G. Tan, P. Yu, L. Zhou, C. Ning, A Tough and Self-Powered Hydrogel for Artificial Skin, Chem. Mater. 31 (2019) 9850–9860, https://doi.org/10.1021/acs.chemmater.9b04041.
[12] Y. Li, Q. Li, X. Zhang, J. Zhang, S. Wang, L. Lai, K. Zhu, W. Liu, Realizing record-high output power in flexible gelatin/GTA-KCl-$FeCN^{4-/3-}$ ionic thermoelectric cells enabled by extending the working temperature range, Energy Envir. Sci. 15 (2022) 5379–5390, https://doi.org/10.1039/d2ee02792e.
[13] C.G. Han, X. Qian, Q. Li, B. Deng, Y. Zhu, Z. Han, W. Zhang, W. Wang, S.P. Feng, G. Chen, W. Liu, Giant thermopower of ionic gelatin near room temperature, Science 368 (2020) 1091–1098, https://doi.org/10.1126/science.aaz5045.
[14] H. Cheng, X. He, Z. Fan, J. Ouyang, Flexible Quasi-Solid State Ionogels with Remarkable Seebeck Coefficient and High Thermoelectric Properties, Adv. Energy Mater. 9 (2019) 1901085, https://doi.org/10.1002/aenm.201901085.
[15] Z. Xu, F. Zhou, H. Yan, G. Gao, H. Li, R. Li, T. Chen, Anti-freezing organohydrogel triboelectric nanogenerator toward highly efficient and flexible human-machine

interaction at −30°C, Nano Energy 90 (2021) 106614, https://doi.org/10.1016/j.nanoen.2021.106614.
[16] P. Nakhanivej, H.H. Rana, H. Kim, B.Y. Xia, H.S. Park, Transport and Durability of Energy Storage Materials Operating at High Temperatures, ACS Nano 14 (7) (2020) 7696–7703, https://doi.org/10.1021/acsnano.0c04402.
[17] X. Liu, O.O. Taiwo, C. Yin, M. Ouyang, R. Chowdhury, B. Wang, H. Wang, B. Wu, N.P. Brandon, Q. Wang, S.J. Cooper, Aligned Ionogel Electrolytes for High-Temperature Supercapacitors, Adv. Sci. 6 (5) (2019) 1801337, https://doi.org/10.1002/advs.201801337.
[18] S. Wu, J. Huang, S. Jing, H. Xie, S. Zhou, Biodegradable Shape-Memory Ionogels as Green and Adaptive Wearable Electronics Toward Physical Rehabilitation, Adv. Funct. Mater. 33 (2023) 2303292, https://doi.org/10.1002/adfm.202303292.
[19] S. Wang, D. Zhang, J. Zhou, X. He, S.Y. Zheng, J. Yang, Zwitterionic ionogels with water-mediated stiffness transition for shape memory and moisture electric generation, Nano Energy 120 (2024) 109166, https://doi.org/10.1016/j.nanoen.2023.109166.
[20] Q. Lyu, S. Wang, B. Peng, X. Chen, S. Du, M. Li, L. Zhang, J. Zhu, Bioinspired Photonic Ionogels as Interactively Visual Ionic Skin with Optical and Electrical Synergy, Small 17 (41) (2021) e2103271.
[21] T. Li, Y. Wang, S. Li, X. Liu, J. Sun, Mechanically Robust, Elastic, and Healable Ionogels for Highly Sensitive Ultra-Durable Ionic Skins, Adv. Mater. 32 (32) (2020) e2002706.
[22] Z. Wang, X. Sun, Z. Guo, R. Xi, L. Xu, Z. Zhao, Y. Ge, Z. Cao, X. Jiang, W. Yang, L. Jiang, Fabrication of submicron linewidth silver grid/ionogel hybrid films for highly stable flexible transparent electrodes via asymmetric wettability template-assisted self-assembly, Chem. Eng. J. 469 (2023) 144065, https://doi.org/10.1016/j.cej.2023.144065.
[23] C. Ma, H. Luo, M. Liu, H. Yang, H. Liu, X. Zhang, L. Jiang, Preparation of intrinsic flexible conductive PEDOT:PSS@ionogel composite film and its application for touch panel, Chem. Eng. J. 425 (2021) 131542, https://doi.org/10.1016/j.cej.2021.131542.
[24] X. Ming, W. Zhong, Y. Ke, J. Lu, K. Jia, X. Ding, H. Jiang, M. Li, D. Wang, Isopropanol-regulated adhesion-controllable conductive gels for robust bioelectric signal monitoring and flexible underwater robots, Chem. Eng. J. 460 (2023) 141746, https://doi.org/10.1016/j.cej.2023.141746.
[25] Y. Fang, H. Cheng, H. He, S. Wang, J. Li, S. Yue, L. Zhang, Z. Du, J. Ouyang, Stretchable and Transparent Ionogels with High Thermoelectric Properties, Adv. Funct. Mater. 30 (2020) 2004699, https://doi.org/10.1002/adfm.202004699.
[26] L. Li, H. Li, J. Wei, R. Li, J. Sun, C. Zhao, T. Chen, w, Polymers (Basel) 15 (2023) 15071746, https://doi.org/10.3390/polym15071746.
[27] Y.H. Pai, J. Tang, Y. Zhao, Z. Liang, Ionic Organic Thermoelectrics with Impressively High Thermopower for Sensitive Heat Harvesting Scenarios, Adv. Energy Mater. 13 (2022) 2202507, https://doi.org/10.1002/aenm.202202507.
[28] Z. Wang, S. Yao, S. Wang, Z. Liu, X. Wan, Q. Hu, Y. Zhao, C. Xiong, L. Li, Self-powered energy harvesting and implantable storage system based on hydrogel-enabled all-solid-state supercapacitor and triboelectric nanogenerator, Chem. Eng. J. 463 (2023) 142427, https://doi.org/10.1016/j.cej.2023.142427.
[29] M. Wang, P. Zhang, M. Shamsi, J.L. Thelen, W. Qian, V.K. Truong, J. Ma, J. Hu, M. D. Dickey, Tough and stretchable ionogels by in situ phase separation, Nat. Mater. 21 (2022) 359–365, https://doi.org/10.1038/s41563-022-01195-4.
[30] J. Wei, Y. Zheng, T. Chen, A fully hydrophobic ionogel enables highly efficient wearable underwater sensors and communicators, Mater. Horiz. 8 (2021) 2761–2770, https://doi.org/10.1039/d1mh00998b.
[31] M. Li, Q. Guan, C. Li, E. Saiz, Self-powered hydrogel sensors, Device 1 (2023) 100007, https://doi.org/10.1016/j.device.2023.100007.
[32] Y. Luo, M. Yu, Y. Zhang, Y. Wang, L. Long, H. Tan, N. Li, L. Xu, J. Xu, Highly sensitive strain sensor and self-powered triboelectric nanogenerator using a fully physical crosslinked double-network conductive hydrogel, Nano Energy 104 (2022) 107855, https://doi.org/10.1016/j.nanoen.2022.107955.
[33] B. Bagchi, P. Datta, C.S. Fernandez, L. Xu, P. Gupta, W. Huang, A.L. David, D. Siassakos, S. Homer-Vanniasinkam, M.K. Tiwari, A stretchable, self-healing and semi-transparent nanogenerator for energy harvesting and sensing, Nano Energy 107 (2023) 108127, https://doi.org/10.1016/j.nanoen.2022.108127.
[34] Q. Li, L. Chen, M. Guo, Z. Hu, Extremely Stretchable and Tough Piezoelectric Gels for Artificial Electronic Skin, Adv. Mater. Technol. 7 (2021) 2101371, https://doi.org/10.1002/admt.202101371.
[35] Y. Dobashi, D. Yao, Y. Petel, T.N. Nguyen, M.S. Sarwar, Y. Thabet, C.L.W. Ng, E. Scabeni Glitz, G.T.M. Nguyen, C. Plesse, F. Vidal, C.A. Michal, J.D.W. Madden, Piezoionic mechanoreceptors: Force-induced current generation in hydrogels, Science 376 (2022) 502-507, https://doi.org/10.1126/science.aaw1974.
[36] M. Du, D. Zhang, W. Fan, K. Zhao, Y. Xia, Z. Nie, K. Sui, Ionic diode-based self-powered ionic skins with multiple sensory capabilities, Mater. Today Phys. 26 (2022) 100744, https://doi.org/10.1016/j.mtphys.2022.100744.
[37] Y. Zhang, C.K. Jeong, J. Wang, X. Chen, K.H. Choi, L.Q. Chen, W. Chen, Q. M. Zhang, Q. Wang, Hydrogel Ionic. Diodes toward Harvesting Ultralow-Frequency Mechanical Energy, Adv. Mater. 33 (2021) e2103056.
[38] L. Chen, J. Lou, X. Rong, Z. Liu, Q. Ding, X. Li, Y. Jiang, X. Ji, W. Han, Super-stretching and high-performance ionic thermoelectric hydrogels based on carboxylated bacterial cellulose coordination for self-powered sensors, Carbohydr. Polym. 321 (2023) 121310, https://doi.org/10.1016/j.carbpol.2023.121310.
[39] X. Li, Z. Tan, B. Guo, C. Yu, M. Yao, L. Liang, X. Wu, Z. Zhao, F. Yao, H. Zhang, S. Lyu, C. Yuan, J. Li, Magnet-oriented hydrogels with mechanical–electrical anisotropy and photothermal antibacterial properties for wound repair and monitoring, Chem. Eng. J. 463 (2023) 142387, https://doi.org/10.1016/j.cej.2023.142387.
[40] C. Liu, S. Wang, X. Wang, J. Mao, Y. Chen, N.X. Fang, S.-P. Feng, Hydrovoltaic energy harvesting from moisture flow using an ionic polymer–hydrogel–carbon composite, Energy Envir. Sci. 15 (2022) 2489–2498, https://doi.org/10.1039/d2ee00030j.
[41] X. Li, X. Xiao, C. Bai, M. Mayer, X. Cui, K. Lin, Y. Li, H. Zhang, J. Chen, Thermogalvanic hydrogels for self-powered temperature monitoring in extreme environments, J. Mater. Chem. C 10 (2022) 13789–13796, https://doi.org/10.1039/d2tc00889k.
[42] C. Bai, Z. Wang, S. Yang, X. Cui, X. Li, Y. Yin, M. Zhang, T. Wang, S. Sang, W. Zhang, H. Zhang, Wearable Electronics Based on the Gel Thermogalvanic Electrolyte for Self-Powered Human Health Monitoring, ACS Appl. Mater. Interfaces 13 (2021) 37316–37322, https://doi.org/10.1021/acsami.1c12443.
[43] B. Siregar, F. Fadli, U. Andayani, L.A. Harahap, F. Fahmi, Monitoring of Solar Radiation Intensity using Wireless Sensor Network for Plant Growing, J. Phys. Conf. Ser. 801 (2017) 012087, https://doi.org/10.1088/1742-6596/801/1/012087.
[44] S. Wang, T. Jiang, Y. Meng, R. Yang, G. Tan, Y. Long, Scalable thermochromic smart windows with passive radiative cooling regulation, Science 374 (2021) 1501–1504, https://doi.org/10.1126/science.abg0291.
[45] W. Gu, P. Zhou, W. Zhang, Z. Luo, L. Chen, Pencil-Drawn Generator Built-in Actuator for Integrated Self-Powered/Visual Dual-Mode Sensing Functions and Rewritable Display, Adv. Sci. 10 (7) (2023) e2206467.
[46] P. Zhou, J. Lin, W. Zhang, Z. Luo, L. Chen, Photo-thermoelectric generator integrated in graphene-based actuator for self-powered sensing function, Nano Res. 15 (6) (2021) 5376–5383, https://doi.org/10.1007/s12274-021-3791-3.
[47] Y.S. Jung, D.H. Jeong, S.B. Kang, F. Kim, M.H. Jeong, K.-S. Lee, J.S. Son, J.M. Baik, J.-S. Kim, K.J. Choi, Wearable solar thermoelectric generator driven by unprecedentedly high temperature difference, Nano Energy 40 (2017) 663–672, https://doi.org/10.1016/j.nanoen.2017.08.061.
[48] J. Shen, Y. Ma, C. Yang, S. Liu, J. Li, Z. Chen, B. Tian, S. Li, Boosting solar-thermal-electric conversion of thermoelectrochemical cells by construction of a carboxymethylcellulose-interpenetrated polyacrylamide network, J. Mater. Chem. A 10 (2022) 7785–7791, https://doi.org/10.1039/d2ta00025c.
[49] H. Yang, S. Ahmed Khan, N. Li, R. Fang, Z. Huang, H. Zhang, Thermogalvanic gel patch for self-powered human motion recognition enabled by photo-thermal-electric conversion, Chem. Eng. J. 473 (2023) 145247, https://doi.org/10.1016/j.cej.2023.145247.
[50] Z. Liu, H. Cheng, Q. Le, R. Chen, J. Li, J. Ouyang, Giant Thermoelectric Properties of Ionogels with Cationic Doping, Adv. Energy Mater. 12 (2022) 2200858, https://doi.org/10.1002/aenm.202200858.